CIMAC CONGRESS 25
ZURICH, MAY 19 – 23, 2025

2025 | 041

Verification of a CFD Model on Hydrogen Combustion in a Large Marine Two-Stroke Engine

Simulation Technologies, Digital Twins and Complex System Simulation

Yudai Abe, Mitsui E&S Co., Ltd.

Tatsuo Suyama, Mitsui E&S Co., Ltd.
Ryosuke Ishibashi, Mitsui E&S Co., Ltd.
Johan Sjöholm, MAN Energy Solutions SE
Simon Ringsted, MAN Energy Solutions SE

ABSTRACT

The IMO's GHG reduction strategy adopted in 2023 sets a goal of achieving net-zero GHG emissions by around 2050, and efforts are underway to commercialize zero-carbon fuels such as hydrogen and ammonia in the maritime sector. In particular, hydrogen, which is the focus of this paper, has the characteristics of extremely high burning velocity and extremely low minimum ignition energy compared to conventional fuels such as heavy fuel oil and natural gas. It is necessary to clarify the applicability of hydrogen in the maritime sector.

MAN Energy Solutions (MAN-ES) and Mitsui E&S (MES) conducted hydrogen-fueled combustion tests using MES's 4S50ME-T, a 4-cylinder, 50 cm bore test engine. 1 cylinder was hydrogen-fueled and the remaining 3 cylinders were MDO-fueled. The hydrogen-fueled cylinder has the same structure and system as the natural gas-fueled ME-GI engine, which is a diffusion combustion system with pilot fuel injection near TDC, followed by injection of high-pressure hydrogen gas. In addition, a premixed combustion system, in which hydrogen gas is injected into the cylinder during the compression process followed by pilot fuel injection at the TDC, was also investigated. Based on the above test results, a simulation model was constructed to reproduce hydrogen combustion by fitting it to a 3-dimensional CFD model.

Unsteady compressible fluid analysis including flow, spray, and combustion was performed using the CFD solver CONVERGE from Convergent Science. Because of the large scale of the calculations, a supercomputer from the Foundation for Computational Science (FOCUS) was used. The sonic speed in hydrogen is much higher than that of natural gas. When using the conventional gas jet method, in which hydrogen is injected as the gas phase, a finer computational grid is required to accurately reproduce the hydrogen jet. However, this leads to a drastic increase in computational load. Therefore, the gas parcel method, in which the entire injected gas is represented by a finite number of representative particles called parcels, was also used as a model for hydrogen injection. The gas parcel method reduces the computation time without increasing the grid size by using parcels to represent the momentum concentration below the computational grid spacing.

Based on the measured data from the combustion tests, the boundary conditions and physical model were adjusted, and a hydrogen combustion simulation model for a large marine two-stroke engine was constructed by fitting the model to a CFD model. Furthermore, by using the gas parcel method, it was confirmed that the accuracy was equivalent to that of the gas jet method and that the computation time could be significantly reduced. This means that a large number of parameter studies are feasible, and the simulation model is expected to be a very effective tool for future research and development of hydrogen combustion optimization.

1 INTRODUCTION

The IMO's GHG reduction strategy adopted in 2023 sets a target of net-zero GHG emissions by around 2050 [1], and efforts are underway in the maritime sector to shift from conventional fossil fuels to the practical use of decarbonized fuels such as hydrogen and ammonia that do not contain carbon atoms and do not emit CO_2 when burned. Among decarbonised fuels, hydrogen has the advantages of being non-toxic and being generated from renewable energy sources, but it has significantly different combustion characteristics from conventional fuels, such as a very high combustion rate and extremely low minimum ignition energy. Addressing the combustion characteristics is one of the challenges in the development of hydrogen-fuelled engines, research and development for two and four stroke marine engines is currently underway [2]. However, there are few reports on combustion tests and numerical simulations using large marine two-stroke engines with a bore diameter of 500 mm or more, which are commonly used as main engines for ocean-going vessels.

Therefore, MAN Energy Solutions (MAN-ES) and Mitsui E&S (MES) conducted a hydrogen combustion test using a test engine 4S50ME-T with a bore diameter of 500 mm to investigate the applicability of hydrogen fuel. MES also conducted numerical simulations using 3D-CFD based on the combustion test results and developed a simulation model to reproduce hydrogen combustion in a cylinder. Simulations were also carried out using the gas parcel method for the hydrogen jet model in order to reduce calculation time. As the speed of sound of hydrogen is much higher than that of natural gas, the conventional method of injecting hydrogen in the gas phase requires a finer computational grid in order to reproduce hydrogen jets with high accuracy. However, this leads to a dramatic increase in computational load. Therefore, a numerical simulation using the gas parcel method, in which the entire injected gas is represented by a finite number of representative particles called parcels, was also carried out as a hydrogen jet model, in an attempt to significantly reduce the calculation time.

In this study, hydrogen combustion characteristics were determined by hydrogen combustion tests using a full-scale engine and a comparison was made between the combustion test results and the numerical simulation results, with the aim of developing a simulation model that can reproduce hydrogen combustion in a large marine two-stroke engine. Numerical simulations were also carried out by applying the gas parcel method to the hydrogen jet model in order to reduce the calculation time.

2 HYDROGEN COMBUSTION

Two combustion types for hydrogen-fuelled marine two-stroke engines were investigated, as shown below.

One is the diffusion combustion type, and its engine cycle is shown in Figure 1. This is the same as the natural gas-fuelled ME-GI, in which pilot diesel oil is injected near the top dead centre to ignite the fuel and hydrogen is injected immediately afterwards to continue combustion. In principle, abnormal combustion such as preignition and knocking does not occur, so stable combustion can be expected. However, as combustion occurs around the theoretical mixing ratio, there is a concern that a large amount of NOx is emitted.

Another combustion type is to inject hydrogen into the cylinder during the compression process and ignite the compressed mixture by pilot injection for combustion. The engine cycle is shown in Figure 2. Although a homogeneous mixture may not be formed depending on the position and direction of the hydrogen injection, this type is hereafter simply referred to as a premixed combustion type. Although homogeneous and lean combustion can suppress NOx emissions, there is concern that abnormal combustion such as knocking and premature ignition may occur.

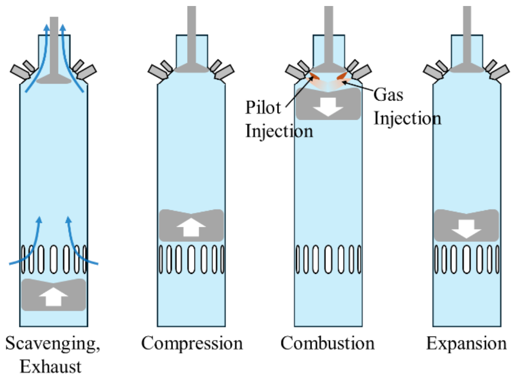

Figure 1. Cycle of diffusion combustion

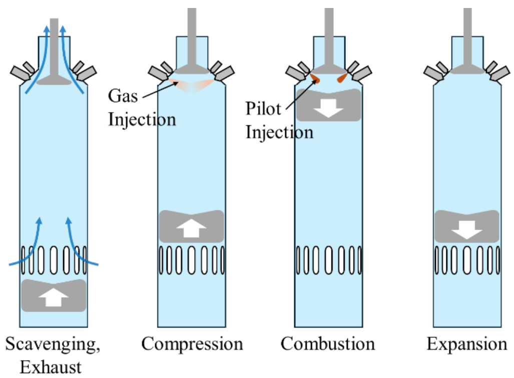

Figure 2. Cycle of premixed combustion

3 COMBUSTION TEST

3.1 Test Engine

When carrying out hydrogen combustion tests, modifications were made to the cylinder cover and peripheral equipment in order to convert one of the four cylinders of our 4S50ME-T9.7 test engine into a hydrogen combustion cylinder. Specifically, the hydrogen gas injection valve, pilot injection valve and gas control block that controls the hydrogen gas supply to the cylinder were added. The cylinder was designed based on the ME-GI, which can use both natural gas and diesel oil as fuel. The upper part of the cylinder of the test engine is shown in Figure 3 and the engine specifications in Table 1.

The hydrogen-fuelled cylinder can be operated in two modes: gas mode, in which hydrogen is used as the main fuel and diesel oil as the pilot fuel, and oil mode, in which only diesel oil is used as fuel. The diesel oil valve, which operates as a pilot valve in the gas mode, operates as the main fuel valve in the oil mode. Cylinders other than the hydrogen-fuelled cylinder were operated in the same way as in a normal diesel oil-fuelled engine. The ME-GI is a diffusion combustion engine, but by adjusting the hydrogen injection timing, combustion tests were carried out for both diffusion and premixed combustion types.

Figure 3. 4S50ME-T9.7

Table 1. Specifications of 4S50ME-T9.7

Specification	
Number of cylinders	4
Bore (mm)	500
Stroke (mm)	2214
Output (kW/Cylinder)	1780
Speed (1/min)	117

3.2 Test Results

3.2.1 Diffusion combustion

Figures 4 and 5 show graphs of in-cylinder pressure and apparent rate of heat release in diffusion combustion at 100 and 75%MCR. MCR refers to Maximum Continuous Rating. For the gas mode, the hydrogen mixing ratio is set at around 90%.The results for the oil mode are also shown. In-cylinder pressures equivalent to those in the oil mode were obtained even in the gas mode with hydrogen as the main fuel, confirming the applicability of the ME-GI-based design to large marine two-stroke engines fuelled with hydrogen.

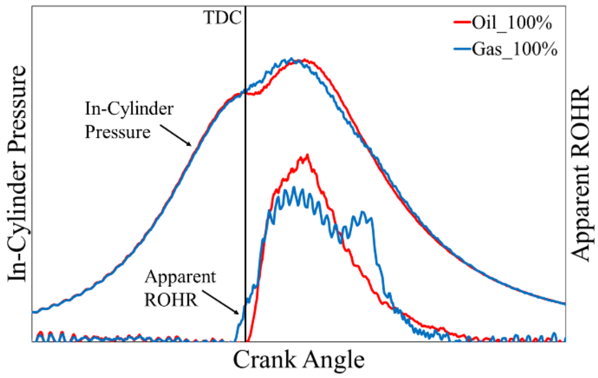

Figure 4. In-cylinder pressure and rate of heat release (Diffusion combustion, 100%MCR)

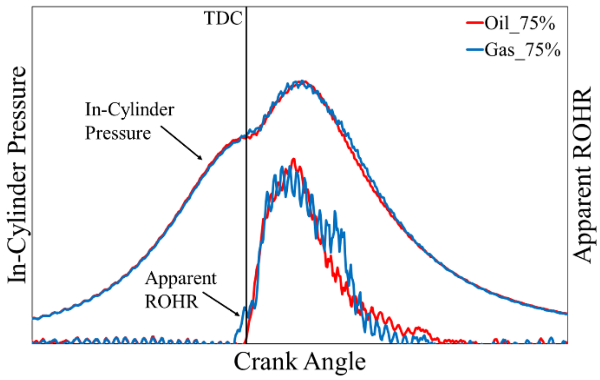

Figure 5. In-cylinder pressure and rate of heat release (Diffusion combustion, 75%MCR)

3.2.2 Premixed combustion

In the premixed combustion test, considering the possibility of preignition, the test was started at a low load of 25%MCR, starting with diesel oil only, and the hydrogen mixing ratio was gradually increased until preignition occurred. Figure 6 shows a graph of in-cylinder pressure and apparent rate of heat release at a hydrogen mixing ratio estimated to be around 5%, where preignition was observed, together with the average value over 20 cycles and the result of one cycle in which preignition was observed. The former shows heat release during pilot injection after top dead centre, while the latter shows heat release during the compression process before top dead centre, indicating preignition. Therefore, it is considered difficult to apply the premixed combustion type to large marine two-stroke engines fuelled with hydrogen, because preignition occurs when even a very small amount of hydrogen is injected during the compression process.

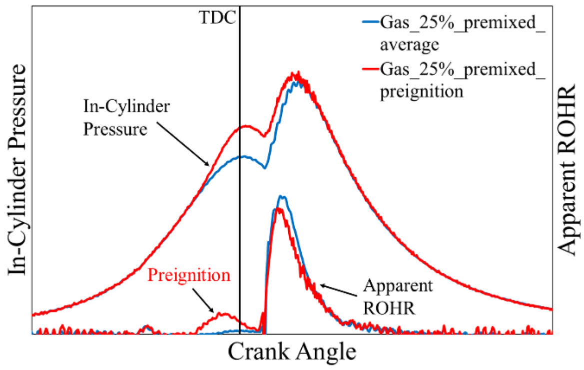

Figure 6. In-cylinder pressure and rate of heat release (Premixed combustion, 25%MCR)

4 NUMERICAL SIMULATION

4.1 Numerical Model

Flow, spray and combustion simulations in a hydrogen-fuelled cylinder were carried out using the general analysis software CONVERGE (Convergent Science). The computational domain is shown in Figure 7. The computational domain extends from the boundary between the scavenging receiver and the cylinder frame, through the cylinder to the exhaust receiver, and is a single-cylinder model with only the hydrogen-fuelled cylinder. The calculation period was one cycle from the opening of the exhaust valve through the scavenging, compression, combustion and expansion stages to the re-opening of the exhaust valve.

Table 2 shows the physical model used. The turbulence calculations were performed by the Reynolds Average Model (RANS) and the RNG k-ε model was used. For the pilot jet, a discrete droplet model (DDM) was used, with the Modified KH-RT model as a sub-model of the DDM for the splitting model and the Frossling model for the evaporation model. The pilot fuel used in the combustion tests is diesel oil. In the simulations, however, to reduce the computational load, the fuel was set to be equivalent to diesel oil when present in droplets and to change to normal heptane (C_7H_{16}) when it evaporates. The coefficients of the thermodynamic function were adjusted so that the lower heating value of C_7H_{16} was equal to that of the diesel oil used in the tests. The combustion model used the detailed chemical reaction solver SAGE, with a merged mechanism of the detailed reaction mechanism Nordin model for C_7H_{16} [4] and the detailed reaction mechanism Zhang model for hydrogen and NOx [5].

The basic size of the computational grid was set to 40 mm. For regions with complex wall geometries and regions where increased flow velocities are expected due to fuel injection, the computational grid was subdivided by Fixed Embedding. The computational grid was also subdivided according to the flow velocity and temperature gradients by Adaptive Mesh Refinement (AMR). An example of a mesh arrangement is shown in Figure 8. The simulation is a transient analysis that takes into account piston and exhaust valve movement, and the number of computational meshes reaches up to 3.6 million, making it a large-scale calculation. For this reason, a supercomputer of Foundation for Computational Science (FOCUS) was used to reduce the computation time.

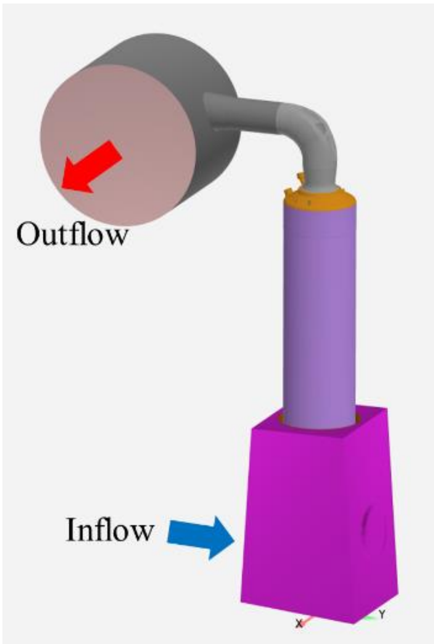

Figure 7. Computation domain

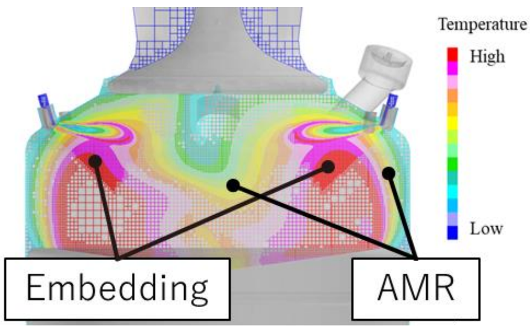

Figure 8. Mesh arrangement

Table 2. Physical model

	Physical model
Turbulence	RNG k-ε model
Droplet breakup	Modified KH-RT model
Combustion	SAGE detailed chemical kinetics solver
Reaction mechanism	Merged mechanism of H_2 and C_7H_{16} (69 Species, 388 Reactions) (H_2 : Zhang, C_7H_{16} : Nordin)

4.2 Boundary and Initial Conditions

The initial conditions and the inflow and outflow boundaries of each area were determined from the measurement data obtained in the combustion tests. Images of the injection of each fuel from the gas and pilot injection valves are shown in Figure 9. The valve geometry is the same for both diffusion and premixed combustion, and both fuels are injected in the swirl direction.

Calculations were carried out for five cases with different operating modes, engine load factors and combustion types. The analysis settings for each case are shown in Table 3. The shapes of the hydrogen and pilot injection rates were deduced from the obtained pressure histories. Figures 10 and 11 show the approximate shapes of the fuel injection rates for 100 and 75%MCR in diffusion combustion. In contrast to the oil mode, the hydrogen fuel in the gas mode is injected at a lower rate and for a longer period of time. The approximate fuel injection rates for 25%MCR in premixed combustion are shown in Figure 12. Hydrogen is injected during the compression process and ignited by pilot injection after passing the top dead centre.

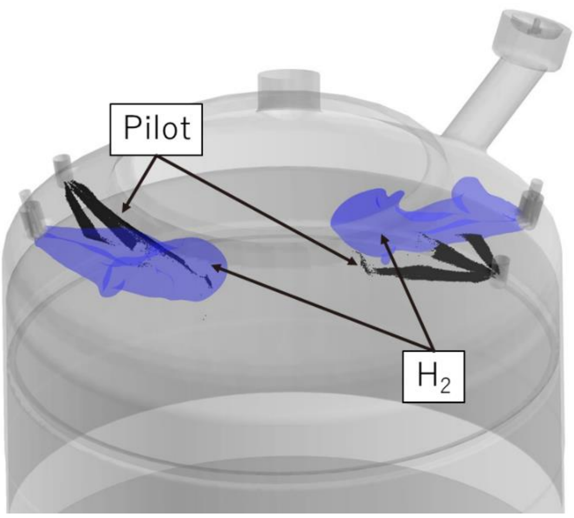

Figure 9. Gas (H_2) injection and pilot injection

Table 3. Setup for each calculation case

Case	Mode	Engine Load (%MCR)	Combustion Type
Oil_100%	Oil	100	Diffusion
Gas_100%	Gas	100	Diffusion
Oil_75%	Oil	75	Diffusion
Gas_75%	Gas	75	Diffusion
Gas_25%_ premixed	Gas	25	Premixed

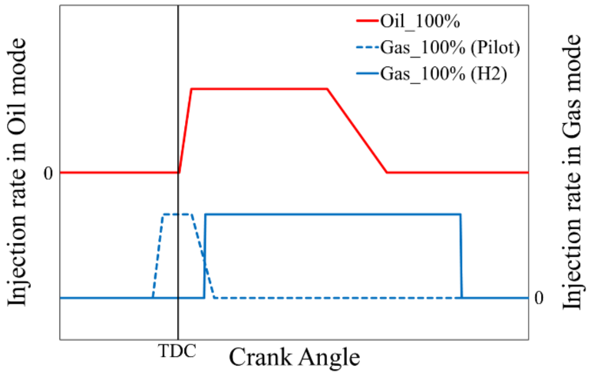

Figure 10. Approximate shape of injection rate (Diffusion combustion, 100%MCR)

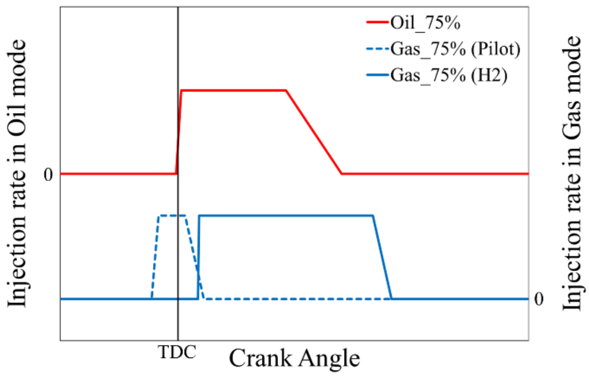

Figure 11. Approximate shape of injection rate (Diffusion combustion, 75%MCR)

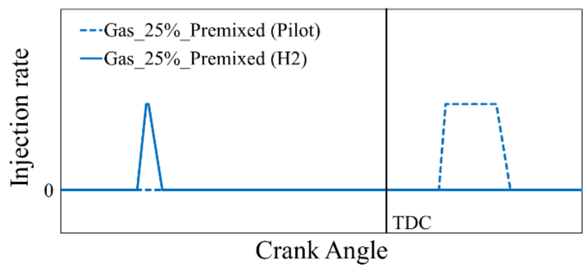

Figure 12. Approximate shape of injection rate (Premixed combustion, 25%MCR)

4.3 Simulation Results

4.3.1 Diffusion combustion

Figures 13 to 16 show the in-cylinder pressure determined from the test results and calculations, and the apparent rate of heat release determined from the in-cylinder pressure. In each case, the calculated results quantitatively reproduce the test results in terms of compression pressure (in-cylinder pressure at top dead centre), maximum pressure, timing of the rise and fall of the rate of heat release and slope.

It was confirmed that the merged mechanism of the Nordin and Zhang models can accurately reproduce the in-cylinder pressure under the test conditions, even under conditions where the main fuel is different, such as oil mode and gas mode. Therefore, it is considered that reasonable calculation results can be obtained even when C_7H_{16} is used as an alternative to diesel oil.

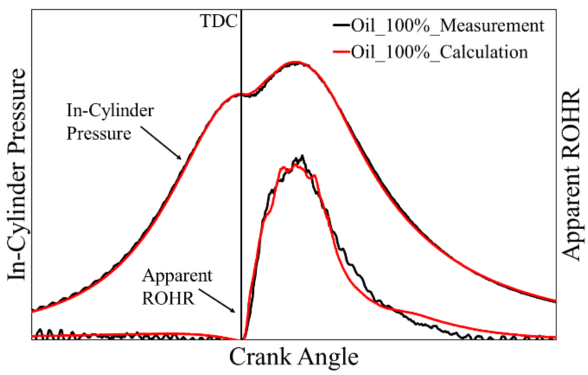

Figure 13. In-cylinder pressure and rate of heat release (Oil mode, 100%MCR)

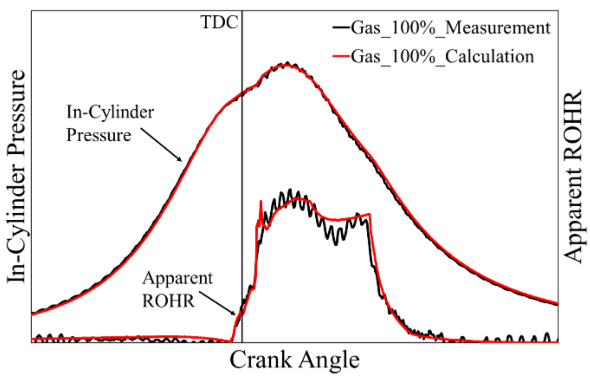

Figure 14. In-cylinder pressure and rate of heat release (Gas mode, 100%MCR)

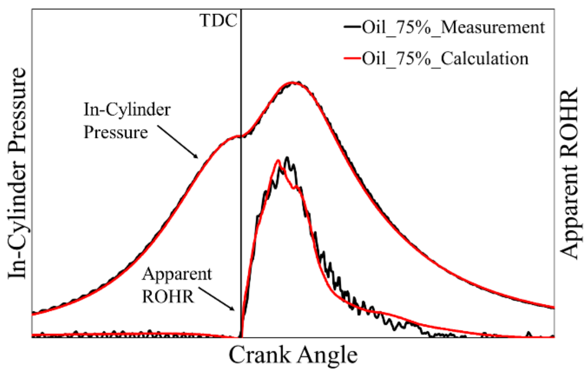

Figure 15. In-cylinder pressure and rate of heat release (Oil mode, 75%MCR)

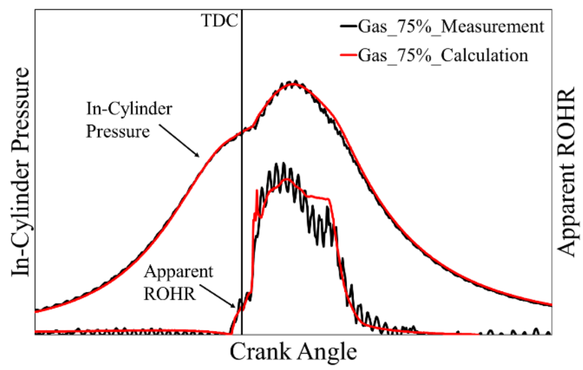

Figure 16. In-cylinder pressure and rate of heat release (Gas mode, 75%MCR)

Figures 17 and 18 show the rate of heat release at each load factor and the ratio Q/Q_f of the integrated heat release rate Q to the calorific value Q_f of the supplied fuel. The rate of heat release shown here is the rate of heat release before subtracting the cooling losses on the combustion chamber walls, and Q/Q_f was also calculated using this. Unlike the apparent rate of heat release in the previous section, this is the rate of heat release obtained during the reaction process of the simulation and cannot therefore be calculated from the test results. In order to focus on the combustion reaction of each fuel, this rate of heat release before subtracting the cooling losses is used here to compare the calculated results for the oil and gas modes.

A comparison of the shape of the rate of heat release for each mode shows that the oil mode has a gradual rise and fall, whereas the gas mode has a steeper rise during the hydrogen injection period. This is thought to be due to the fact that the premixed gas formed during the period before the hydrogen jet reaches the high temperature field caused by the pilot fuel combustion burns rapidly upon ignition. The burning velocity of hydrogen is higher than that of diesel oil at this time, which is thought to be responsible for the rapid increase in the rate of heat release.

The ratio Q/Q_f of the integrated heat release to the heat supplied is compared, focusing on the crank angle CA95% where Q/Q_f = 95% is reached. Figures 10 and 11 show that the fuel injection period is set longer in the gas mode than in the oil mode, but combustion is completed earlier in the gas mode than in the oil mode at both load rates. This suggests that hydrogen burns more rapidly after being injected into the cylinder than diesel oil, with very little afterburning.

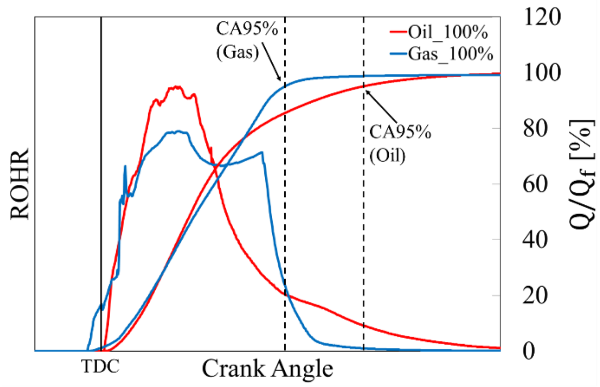

Figure 17. Rate of heat release and Q/Q_f (100%MCR)

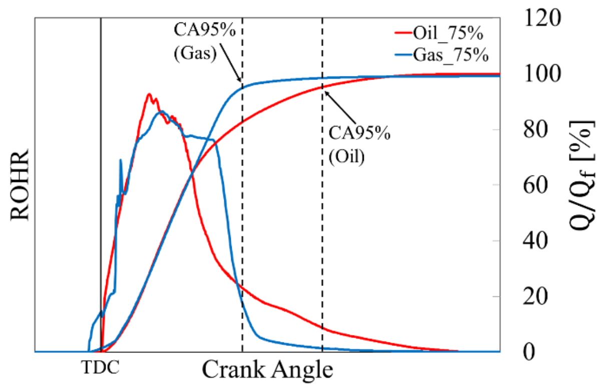

Figure 18. Rate of heat release and Q/Q_f (75%MCR)

Figure 19 shows the indicated thermal efficiency and engine load factor. Here, the indicated thermal efficiencies are normalised by the measured values at 100%MCR in oil mode. Both the test and calculation results show that the indicated thermal efficiency is higher in the gas mode than in the oil mode at each engine load factor. This is considered to be due to the lower afterburning in the gas mode and higher degree of constant volume in the late combustion phase compared to the oil mode. The indicated thermal efficiency was lower for 100% MCR than for 75%MCR in each operating mode. The NOx concentration and engine load factor are shown in Figure 20. Here, the NOx concentration is converted so that the O2 concentration is 13%. As with the indicated thermal efficiency, it is normalised by the measured 100% MCR in oil mode. Both the test and calculation results show that NOx concentration are higher in the gas mode at each engine load factor and in the 100%MCR at each operation mode. The simulation model therefore reproduced the qualitative trends in indicated thermal efficiency and NOx concentration for different operating modes and engine load factors.

Figures 21 and 22 show the mass fractions of the calculated grid above 2500K in the combustion chamber. It can be seen that in both load factors, a higher fraction of the combustion gas in the gas mode is hotter than in the oil mode above 2500K, indicating that the environment is more prone to the generation of thermal NO. This is thought to be due to the fact that hydrogen burns more rapidly than diesel oil after fuel injection, which raises the temperature of the combustion gas and accelerates the generation of thermal NO. The above results show that hydrogen-fuelled engines are more efficient than diesel oil-fuelled engines, but also emit more NOx due to their combustion characteristics.

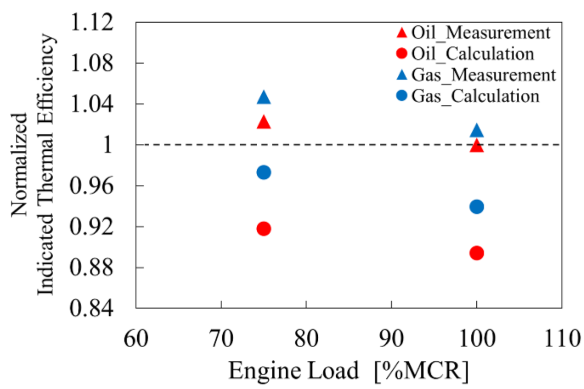

Figure 19. Indicated thermal efficiency

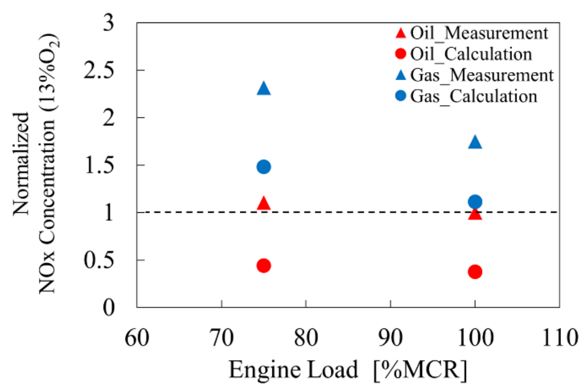

Figure 20. NOx concentration

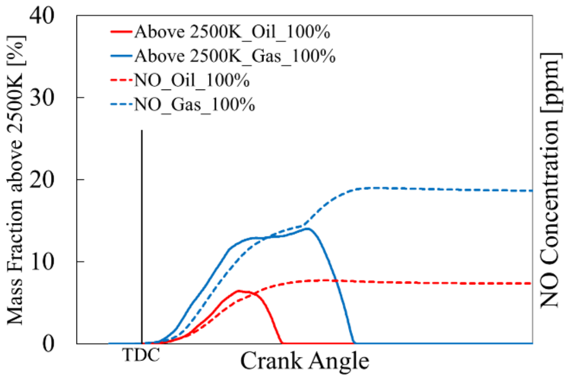

Figure 21. Mass fraction of combustion chamber above 2500K and NO concentration (100%MCR)

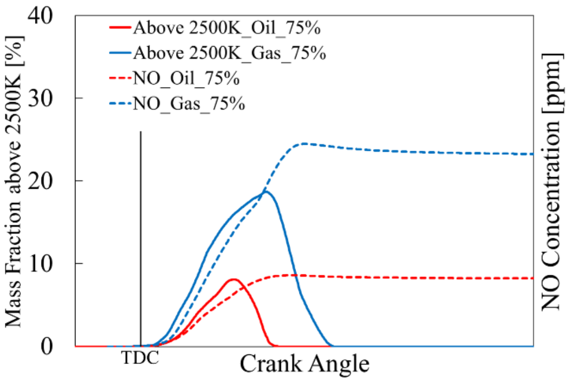

Figure 22. Mass fraction of combustion chamber above 2500K and NO concentration (75%MCR)

4.3.2 Premixed combustion

Figure 23 shows the in-cylinder pressure and apparent rate of heat release in premixed combustion. The calculated results show that ignition does not occur during the compression process and the pressure history is close to the average value of the actual measurements. The rate of heat release was also found to begin to increase at the same time as the average value of the actual measurements. This suggests that the preignition that often occurred in actual measurements was not due to self-ignition of the hydrogen itself. Cylinder oil is supplied to the combustion chamber from the cylinder liner wall, which may have been the source of ignition of the hydrogen.

Figure 24 shows the hydrogen concentration distribution and temperature distribution in the cross-section including the gas injection valve, showing that the hydrogen injected from the gas injection valve swirls and diffuses in the direction of the swirl flow, and the two hydrogen jets mix with the ambient air without interfering with each other. It can be seen that the pilot fuel is then injected and the flame spreads throughout the cylinder.

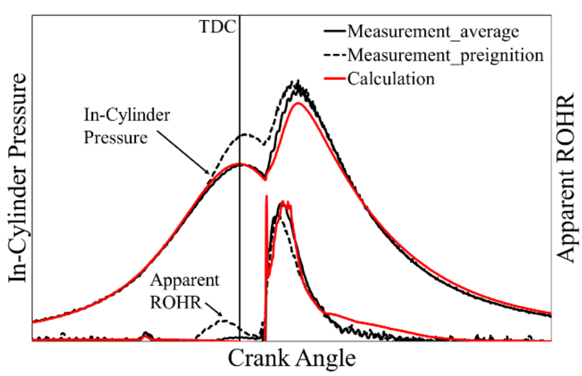

Figure 23. In-cylinder pressure and rate of heat release (Gas mode, 25%MCR, Premixed, Hydrogen mixing ratio 5%)

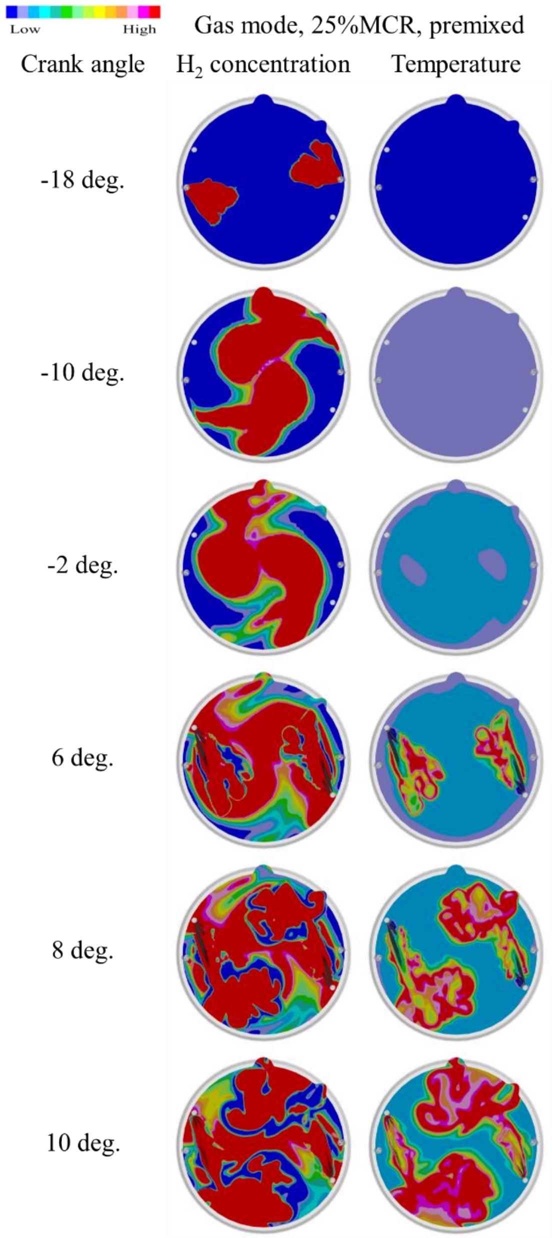

Figure 24. H_2 concentration and temperature distribution (Hydrogen mixing ratio 5%)

5 GAS PARCEL METHOD

5.1 Gas Parcel Method

The gas parcel method is a calculation method for gas jets proposed by Fujimoto et al [3], to represent momentum concentrations that cannot be mesh-resolved.

The gas parcel calculation method applies the discrete droplet model to the consideration of local momentum in jet calculations. In other words, the entire gas jet is represented by a finite number of representative particles called parcels. Each parcel consists of a number of gas particles of equal position, velocity, radius, mass and temperature. The equation of motion is calculated for each parcel and its effect on the gas phase is evaluated by multiplying the quantity per particle by the number of particles constituting the parcel. Concentration diffusion and other phenomena other than momentum are calculated only on the gas phase side.

In conventional calculation methods for gas jets (hereinafter referred to as the gas jet method), when gas is injected from a nozzle, a local momentum concentration occurs near the jet opening, but in order to reproduce this, the mesh must be subdivided down to the jet diameter. In particular, if the jet diameter is relatively small in relation to the analysis area, a significant increase in calculation costs is feared. However, the gas parcel method uses parcels to represent the gas, so even if a coarse mesh is used relative to the jet diameter, the calculation time can be reduced while maintaining accuracy.

The behaviour of each parcels in the gas parcel method is determined by the following equations of motion:

$$\frac{du_d}{dt} = -\frac{1}{\rho_d}\nabla P + \frac{3C_d\rho_g}{4\rho_d d_d}\left|u_g - u_d\right|\left(u_g - u_d\right) - C_{am}\frac{\rho_g}{\rho_d}\frac{d\left(u_d - u_g\right)}{dt} + \frac{\rho_d - \rho_g}{\rho_d}g \qquad (1)$$

where u_d is gas parcel velocity, u_g is gas phase velocity, ρ_d is gas parcel density, ρ_g is gas phase density, d_d is gas parcel diameter, P is pressure, g is gravitational acceleration, C_d is drag coefficient, C_{am} is virtual mass coefficient. If the relative velocity with the gas phase is below the threshold value, the difference in momentum between the parcel and the gas phase becomes small and the interaction with the gas phase becomes small, so the parcel is removed from the calculation.

5.2 Numerical Setup

In this calculation, the gas parcel method was applied by using the User Defined Function (UDF) extension of CONVERGE. In order to use the gas parcel method, it is necessary to set physical properties such as density under the assumed pressure in the gas parcel placed at the outlet of the jet. However, the injection of high-pressure gas causes under-expansion at the jet outlet, and it is difficult to theoretically calculate the pressure in this under-expanded state. For this reason, the static pressure at the jet outlet of the gas jet valve obtained by the gas jet method described in the previous chapter was adopted in this calculation, and the physical property values of hydrogen at this static pressure were used. A contraction factor was set so that the flow velocity at the jet outlet matched the results of the gas jet method calculations.

For the calculation grid, as shown in Figure 25, the calculation grid around the gas jet valve was set coarser than for the gas jet method calculation in the previous chapter to reduce calculation time.

Calculations using the gas parcel method were carried out for two cases with different engine load factors for the diffusion combustion system, as shown in Table 4. The state of the computation domain before the start of hydrogen injection is the same as in the calculation by the gas jet method, so the restart calculation was carried out from before top dead centre.

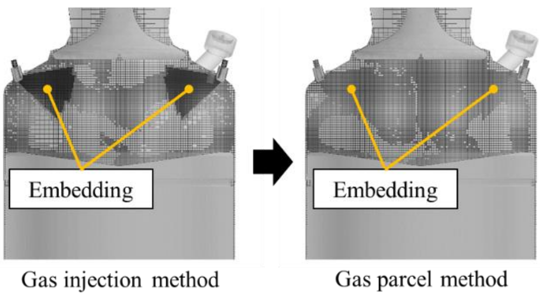

Figure 25. Coarsening of the mesh around gas injection valves

Table 4. Setup for each calculation case

Case	Mode	Engine Load (%MCR)	Combustion Type
GasParcel_ 100%	Gas	100	Diffusion
GasParcel_ 75%	Gas	75	Diffusion

5.3 Simulation Results

Figures 26 and 27 show the in-cylinder pressure and apparent rate of heat release for each engine load factor. It was confirmed that the gas parcel method could approximately reproduce the results of the conventional gas jet calculation in terms of maximum in-cylinder pressure and timing of heat release.

Figures 28 and 29 show the rate of heat release at each engine load factor and the ratio Q/Q_f of the integrated heat release Q to the supplied fuel heat quantity Q_f. It can be seen here that the timing of the rise and fall of heat release can be reproduced. However, a spike in heat release immediately after hydrogen injection and an increase in the rate of heat release in the second half of the hydrogen injection period are observed. A comparison of Q/Q_f shows that the gas parcel method burns out slightly faster.

Figures 30 and 31 show the temperature distribution in the cross-section including gas injection valve for the gas jet and gas parcel methods for each engine load factor. It can be seen that the shape of the temperature distribution immediately after hydrogen injection is approximately the same, but the penetration distance of the gas parcel method gradually becomes shorter than that of the gas jet method, and the jet stream cohesion also becomes uneven. Therefore, it is considered that the rate of heat release in the second half of the hydrogen injection period is larger for the gas parcel method because the variation in the cohesion of the jets accumulates as time passes after the start of hydrogen injection, and the flame area increases.

Figures 32 and 33 show the mass fraction above 2500K and the NO concentration in the combustion chamber for each engine load factor. It can be seen that the gas parcel method produces slightly more high temperature fields above 2500K, with a corresponding increase in NO concentration. As mentioned above, the gas parcel method is considered to produce more rapid combustion in the second half of the hydrogen injection period, resulting in an increase in the high-temperature combustion gases.

In the present calculation, the flow velocity at the jet outlet was set to match that calculated by the gas jet method, but more detailed adjustment of the flow contraction coefficient is considered necessary to reproduce the behaviour of the entire jet. The shape of the jet is expected to be improved by adjusting the assumed pressure and temperature of the gas parcel properties as well, but this is a subject for future work.

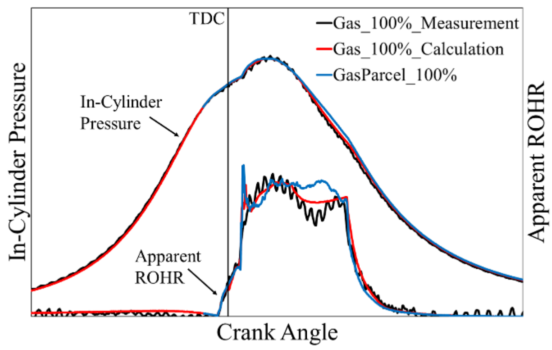

Figure 26. In-cylinder pressure and rate of heat release (Gas mode, 100%MCR)

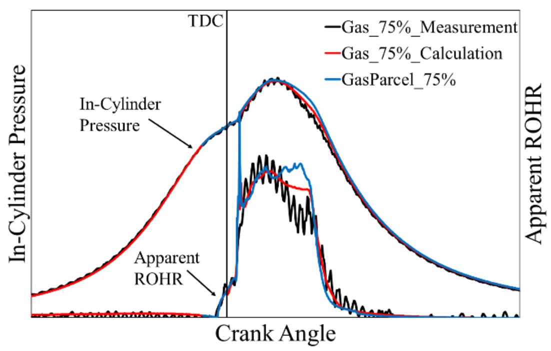

Figure 27. In-cylinder pressure and rate of heat release (Gas mode, 75%MCR)

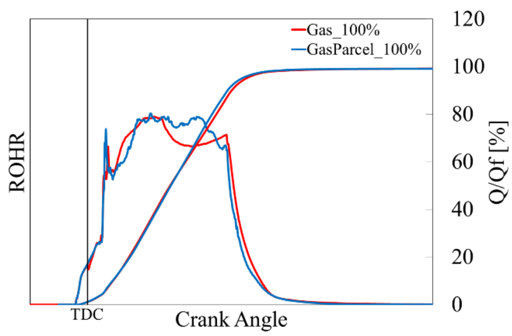

Figure 28. Rate of heat release and Q/Q_f (100%MCR)

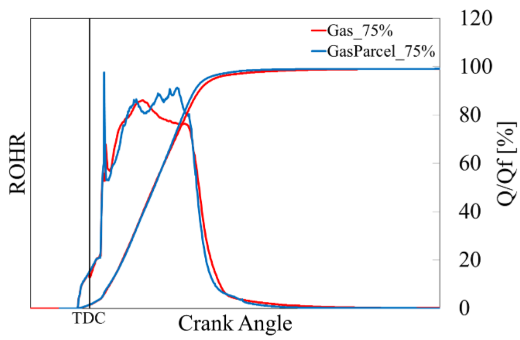

Figure 29. Rate of heat release and Q/Q_f (75%MCR)

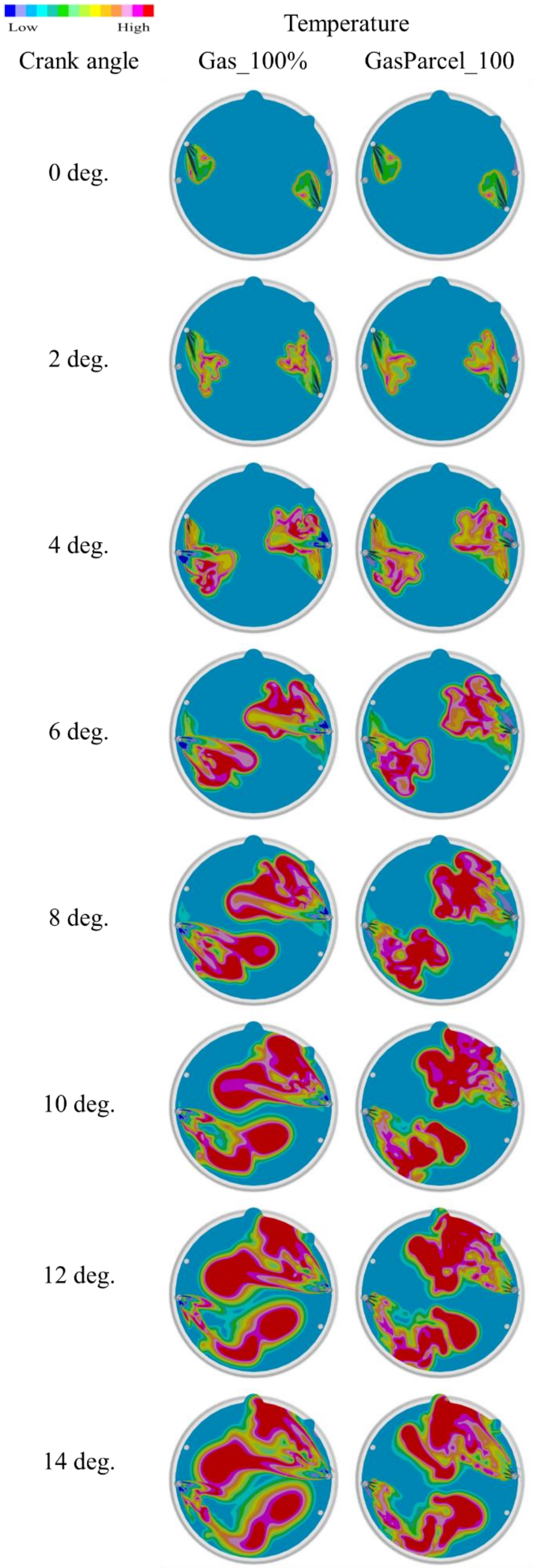

Figure 30. Temperature distribution (100%MCR)

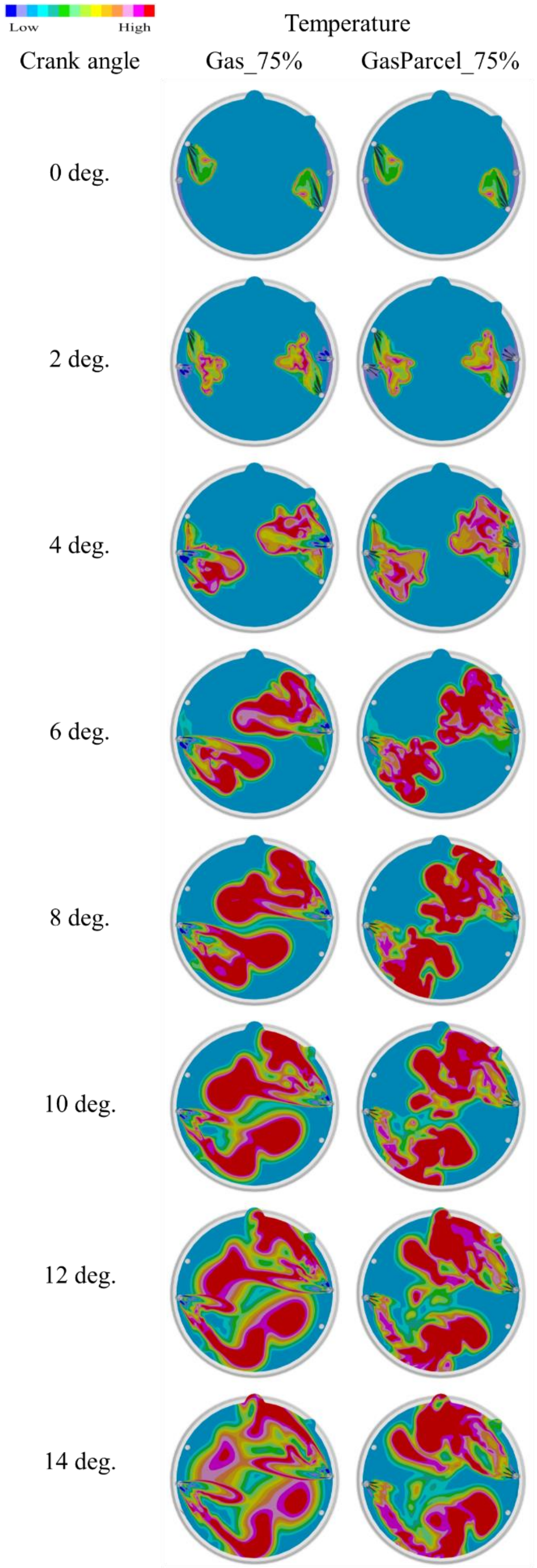

Figure 31. Temperature distribution (75%MCR)

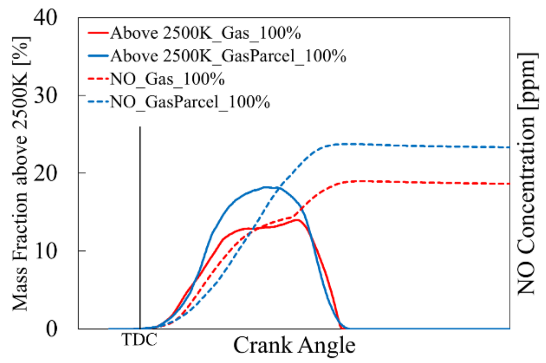

Figure 32. Mass fraction of combustion chamber above 2500K and NO concentration (100%MCR)

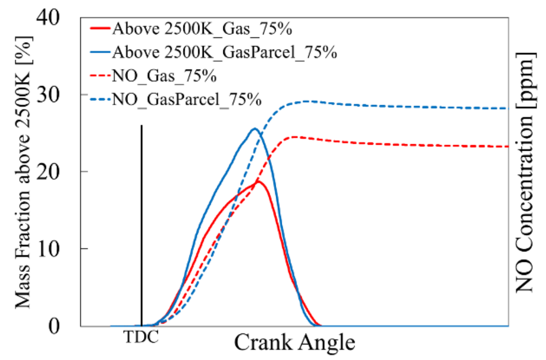

Figure 33. Mass fraction of combustion chamber above 2500K and NO concentration (75%MCR)

5.4 Calculation Time

Table 5 compares the calculation time for each case and Figures 34 and 35 show the history of calculation times at each engine load factor. In the case of the gas jet method, the gas injection period accounts for most of the calculation time, indicating that the calculation of the gas jet is burdensome. In the case of the gas parcel method, however, the calculation time for the gas injection period is significantly reduced to less than one third of that for the gas jet method. Therefore, it was confirmed that the calculation time can be significantly reduced by using the gas parcel method for the calculation of hydrogen jets while maintaining a certain level of calculation accuracy.

Table 5. Calculation time for each calculation case

Case	Gas injection period (h)	After the start of gas injection (h)
Gas_100%	50.79	73.44
GasParcel_100%	15.01	36.02
Gas_75%	41.52	65.79
GasParcel_75%	11.24	33.83

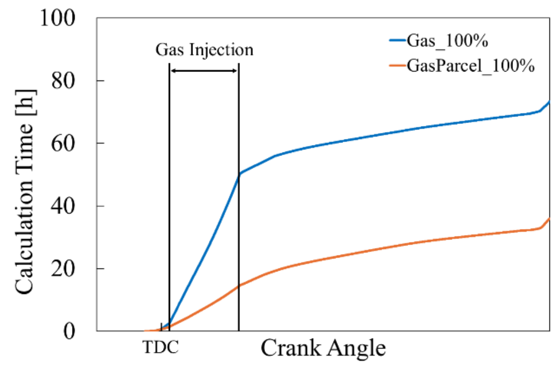

Figure 34. Calculation time (100%MCR)

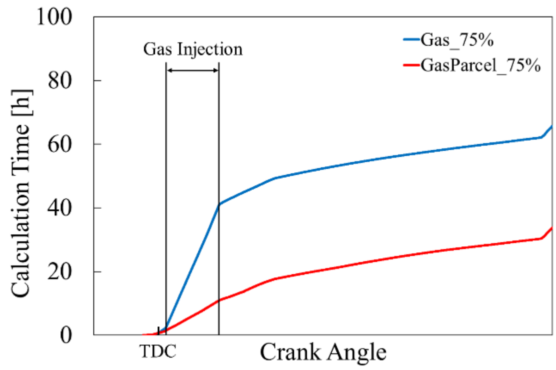

Figure 35. Calculation time (75%MCR)

6 CONCLUSIONS

In this paper, the results of a hydrogen combustion test on a large marine two-stroke engine are compared with the results of a numerical simulation using 3D-CFD to validate the accuracy of the simulation model. Numerical simulations were also carried out by applying the gas parcel method to the hydrogen injection model in order to reduce the calculation time, and the effectiveness of this method in reducing the calculation time was verified.

- The simulation model built on the results of the combustion tests was found to reproduce the test results quantitatively for cylinder pressure and rate of heat release, and qualitatively for thermal efficiency and NOx emissions.
- Hydrogen burns more rapidly after fuel injection than diesel oil, resulting in less afterburning. Therefore, hydrogen-fuelled engines have an advantage in terms of thermal efficiency, but the combustion temperature is higher, and more thermal NO is produced, requiring measures to reduce NOx emissions.
- In the case of premixed combustion type, the results of numerical simulations suggest that the preignition that occurred in the combustion

test was not caused by the auto-ignition of hydrogen itself, but by cylinder oil or other substances.

- It was found that the gas parcel method can reproduce the in-cylinder pressure, rate of heat release, etc. using the conventional gas jet method, and that the calculation time for the hydrogen injection period can be reduced to less than one-third of that using the conventional gas jet method.

In the future, case studies using the gas parcel method will be used to improve the efficiency of specification studies in order to realise high efficiency and low NOx emissions in hydrogen-fuelled engines.

7 DEFINITIONS, ACRONYMS, ABBREVIATIONS

IMO International Maritime Organization

GHG Greenhouse Gas

ME-GI Two-stroke MAN B&W dual fuel engine

MCR Maximum Continuous Ratio

RANS Reynolds Average Model

DDM Discrete Droplet Model

AMR Adaptive Mesh Refinement

ROHR Rate of Heat Release

8 ACKNOWLEDGMENTS

This study was funded by Ministry of Land, Infrastructure, Transport and Tourism in Japan.

9 REFERENCES AND BIBLIOGRAPHY

[1] IMO. 2023. 2023 IMO strategy on reduction of GHG emissions from ships, *MEPC 80*, London, MEPC 80/WP.12, Annex 1.

[2] Takasaki, K., Kawauchi S. and Tsuru D. 2023. Progress and prospect of combustion studies on low- and zero-carbon fuels, *CIMAC Congress 2023*, Busan, Paper No.103.

[3] Fujimoto, H., Takada, Y. and Wakisaka, T. 2007. Proposal of gas parcel method for improving accuracy of gas jet analysis in gas fuel injection engines, *Journal of the JIME*, 42(4): 197-202.

[4] Nordin, N. 1998. Numerical simulations of non-steady spray combustion using a detailed chemistry approach, Thesis for the degree of licentiate of engineering, Dept. of Thermo and Fluid Dynamics, *Chalmers University of Technology*.

[5] Zhang, Y., Mathieu, O., Petersen, E.L., Bourque, G. and Curran, H.J. 2017. Assessing the predictions of a NOx kinetic mechanism using recent hydrogen and syngas experimental data, *Combustion and Flame*,182: 122-141.